Proceedings of the 11th Brazilian Congress of Thermal Sciences and Engineering -- ENCIT 2006
Braz. Soc. of Mechanical Sciences and Engineering -- ABCM, Curitiba, Brazil,- Dec. 5-8, 2006

Paper CIT06-0264

A METHODOLOGY FOR GASEOUS EMISSIONS PREDICTION OF IRON ORE SINTERING BED USING PROCESS DATA

Rogério Ramos
Universidade Federal do Espírito Santo - UFES - Departamento de Engenharia Mecânica
Av. Fernando Ferrari, 514, Goiabeiras, Vitória, ES CEP 2075-910
ramosrogerio@hotmail.com

Roger Hudson Braga Silva
Petróleo Brasileiro S/A.- Petrobras
Av. Elias Agostinho, 665, Imbetiba, Macaé, RJ CEP 27913-350
rhbs@petrobras.com.br

Abstract. *In the present work it is proposed and tested a model for gaseous emissions prediction in a Dwight-Lloyd iron ore sintering bed, utilized to obtain sinter for steelmaking industry. The emissions are modeled using a simulated thermal profile passing through a bed mix constituted by coke, anthracite, iron ore and fluxing, provoking the reactions for the combustion process. Such process is simulated by a chemical equilibrium model generating 10 gaseous species. The emissions so obtained are adjusted for the effectively measured emissions data from Companhia Siderúrgica de Tubarão - CST. This adjustment process is proceded using an approaching parameter associated to the excess air of combustion. Once the adjustment parameter is calculated for the emission in a given production week, this parameter is utilized for the prediction of emissions for subsequent weeks, considering the variation in the mix composition, which is known in advance. In this work the predictions quality is evaluated, when compared to the measured emissions to four weeks in advance.*

Keywords*: Iron Ore Sintering, Dwight-Lloyd, gaseous emissions*

1. Introduction

The process involving the well known iron ore sintering reach great importance in the brazilian industrial scenario, being a heat and mass transfer process very well studied, although the complexity involving the solutions are considerable due to the rug quantity of variables.

The attainment of steel consists of 5 main stages transform operations involving metal works and mechanical resignation according to with Dias (1998). Being the sintering a process that consists basically of mixture and homogenization of a group of ores, fluxing (limestone fine) and materials from the own production process (recycled) with inadequate pellet dimensions for direct use in the blast furnace. This mixture (mix) is burned in a moving bed type furnace called sintering machine.

The objective of this work is to present a methodology for prediction gaseous emissions generated in sintering process, considering thermo-mechanical effects and a large number of actual parameters involved in the process, including temperature of gas and solids, concentration of various gaseous species, bed characteristics like porosity, density, thermal conductivity, beyond operational parameters like dimensions of sintering machine, bed velocity, gas exhaust rate, among others.

The thermal profile was obtained for a very approximated case, using a simple mathematical approach to a linear model of moving heat source problem, with the objective to obtain a typical "thermal wave" like those encountered in such sintering process, but avoiding the non-linear calculation of energy variation due to combustion.

The model for gas generation is simulated by chemical equilibrium approach for 10 (ten) gas species, using the thermal profile described before and process data from the Dwight-Lloyd sintering unit of *Companhia Siderúrgica de Tubarão - CST*.

The temperature and the chemical equilibrium models are validated by comparison with data from open literature.

The proposed methodology is based on a parameter adjustment considering the emissions monitored by the company, *CO* and NO_x, in a given date. Such adjustment is used in the proposed prediction model for a later date. Such predictions are checked against the actual emissions in that date.

2. Bibliographical revision

A literature revision reveals the work of Muchi and Higuchi (1972) as an earlier approach that modeled the iron ore sintering problem just containing combustion and drying process. At same days, Hamada et al. (1972) considered this model, together with calcinations and fusion process. Dash and Rose (1976) presented a model to sintering simulation including drying and condensation inside the bed and considering the limestone reduction in an endothermic reaction with minor relevance in the total energy estimated. Still in the 70's , Young (1977) presented a similar model using the same heat and mass transfer process, but using better numerical techniques. In that case, it was used the predictor-

corrector Adams-Mouton method with initial values obtained from the Euler method. It was estimated the effects of main parameters variation in sintering process. It was introduced the calculation of pressure drop in the bed as well.

Yoshinaga and Kubo (1978) included the void fraction and particle diameter calculation for three distinct zones and Toda and Kato (1984) considered a interface progression rate of the fusing grain added to size distribution of the coke, but the model considered limited chemical reactions and constant properties with temperature variation. Cumming and Thurlby (1990) in a very well detailed model describing the physical-chemical process involved in the process together with the variations of bed characteristics like particle diameter, void fractions (porosity), channeling factor, bed shrinkage. The work reaches good agreement between flux and bed pressure drop, using Ergun equation.

Nath *et al.* (1997) developed a two-dimensional transient model including 11 chemical reactions in a kinetic reactions model applied to the sintering unit of *Companhia Siderúrgica Nacional - CSN*. The model may be used to optimize thermal efficiency and productivity of sintering plants.

3. Chemical equilibrium combustion model

Chemical equilibrium can be resumed as the supposition that a diatomic gas is burned inside a closed, rigid and isolated container. Taking the following concepts:

- Due to the temperature elevation, the consequence of the growing in the average velocity is the growing of the shocks between atoms;
- The consequence is the elevation of the energy level;
- Dissociation occurs, when this energy exceeds the attraction force between the atoms of a molecule, Eq. (1).

$$H_2 \rightarrow 2H \tag{1}$$

- Continuous shocks in appropriated conditions, lead back the dissociated atoms to restore the original molecule, Eq. (2).

$$2H \rightarrow H_2 \tag{2}$$

When hydrogen is burned, and the level of activity of all atomic movements increases, more molecules will be in dissociation condition than associating atoms. With increasing temperature, the amount of molecules of hydrogen will decrease, while the amount of atoms of hydrogen will increase. If temperature decreases, the effect is exactly the opposite. Due to the high collision rate, a steady state is quickly reached.

3. 1. Action Mass Law

The Action Mass Law is a requirement used by Campbell (1979) to define if a system is in chemical equilibrium state, i.e., the situation when the rate of associations and dissociations are equivalents and being a constant product of the system (in the present case, the combustion). It is defined in Eq. (3) to a system composed by 5 gas species, being one specie inert.

$$K_p = \frac{p_3^{v_3} p_4^{v_4}}{p_1^{v_1} p_2^{v_2}} \tag{3}$$

Campbell (1979) obtained a functional relation between Kp and T, using the Kp value computed from the Eq. (3) and the coefficients for various reversible reactions were estimated to apply in expression for Kp as pointed out in Eq. (4) and Table (1) for 10 gas species reacting.

$$K_p = exp\left[\frac{a}{T} + \left(b + \frac{c}{T}\right) * ln(T) + d\right] \tag{4}$$

Table 1 - Coefficients to compute the reaction constant K_p in Eq. (4)

Rection	a	b	c	d
$H_2 + \frac{1}{2} O_2 \leftrightarrow H_2O$	42450.0	-1.0740	-2147.0	3.2515
$CO + \frac{1}{2} O_2 \leftrightarrow CO_2$	33805.0	0.7422	165.8	-16.5739
$2H \leftrightarrow H_2$	33587.0	0.5604	3327.0	-20.8683
$2O \leftrightarrow O_2$	57126.0	-0.0100	599.0	-16.3201
$2H + O \leftrightarrow H_2O$	104702.0	-0.5181	1480.0	-25.8073
$O + H \leftrightarrow OH$	44216.0	-0.1319	1298.0	-13.1303
$CO + H_2O \leftrightarrow CO_2 + H_2$	-8645.0	1.8162	2312.0	-19.8254
$O_2 + N_2 \leftrightarrow 2NO$	-14096.0	-0.6893	-1375.3	9.668
$2N \leftrightarrow N_2$	108142.0	-1.744	-3558.2	0.595
Valid for 1600 < T < 6000 K. Pressure in atmospheres.				

This formulation allows the computation of 10 species of combustion products from chemical equilibrium hypothesis. It was deduced by Campbell (1979) and now it is used to estimate the production of gases originated by the iron ore sintering process, defining a problem as can be seen in Eq. (5).

$$N(1)CO_2 + N(2)CO + N(3)O_2 + N(4)O + N(5)NO + N(6)N_2 + N(7)H + N(8)H_2 + N(9)OH + N(10)H_2O \qquad (5)$$

Considering a fuel composed by carbon, hydrogen, oxygen and nitrogen (known as C/H/O/N fuel) it is needed 10 equations to determine the 10 gaseous species for the combustion products. From the Mass Conservation Law it was getting 4 equations for the fuel atoms species e the others come from Mass Action Law as shown in Tab. (2), making p = 1 to 6.

Table 2 - Equations to compute 10 gaseous species for combustion products

$$\left.\begin{aligned}
&\text{(a)AC} = N(1) + N(2)\\
&\text{(b)W1} = \frac{N(1)}{(N(2) * \sqrt{N(3)})}\\
&\text{(c)W2} = \frac{N(3)}{N(4)^2}\\
&\text{(d)AN} = N(5) + 2N(6)\\
&\text{(e)K3} = \frac{N(5)^2}{(N(3) * N(6))}\\
&\text{(f)AO} = 2[N(1) + N(3)] + N(2) + N(4) + N(5) + N(9) + N(10)\\
&\text{(g)AH} = 2[N(8) + N(10)] + N(7) + N(9)\\
&\text{(h)W4} = \frac{N(8)}{N(7)^2}\\
&\text{(i)W5} = \frac{N(9)}{(N(4) * N(7))}\\
&\text{(j)W6} = \frac{N(10)}{(N(8) * \sqrt{N(3)})}
\end{aligned}\right\}$$

where,

$$\left.\begin{aligned}
&W1 = K1 * (P/NT)1/2\\
&W2 = K2 * P/NT\\
&W4 = K4 * P/NT\\
&W5 = K5 * P/NT\\
&W6 = K6 * (P/NT)1/2
\end{aligned}\right\}$$

and *AC*, *AH*, *AO* and *AN* represents the stoichiometric abundances of carbon, hydrogen, oxygen and nitrogen, respectively, expressed in moles.

3. 2. Checking the emissions model

In order to check the code written for the present study, it was simulated the case presented by Campbell (1979). The comparison can be seen in Fig. (1a,b).

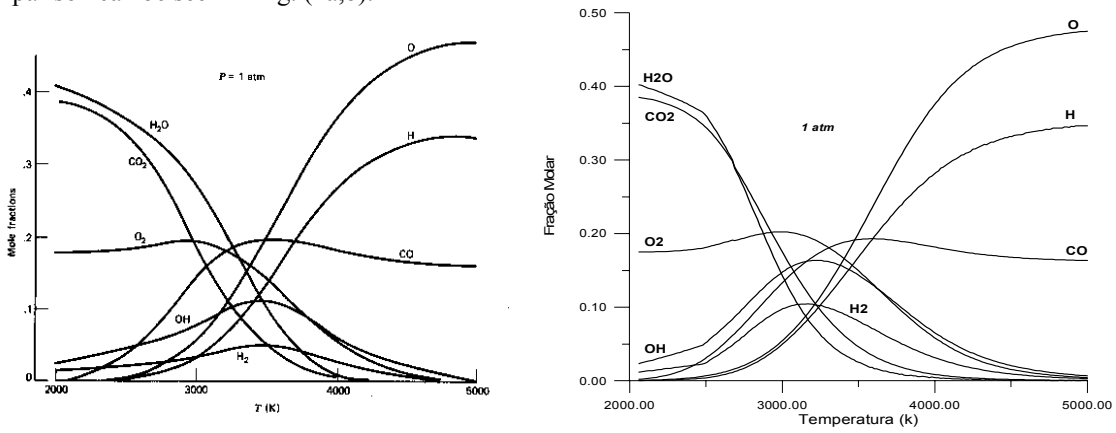

(a) (b)

Figure 1 - (a) Combustion products concentration obtained by chemical equilibrium apporach, by Campbell (1979); (b) Combustion products concentration calculated by the present code. (AC/AH/AO/AN = 10/22/40/0)

As observed in Figs. (1a,b), the concentrations of combustion products that are plotted in both figures reach great concordance to any gas specie plotted at any temperature in the graph.

4. TheThermal Profile Model

The dimensionless domain definitions, the coordinate system and boundary conditions for the sintering bed model are demonstrated in Fig.(2).

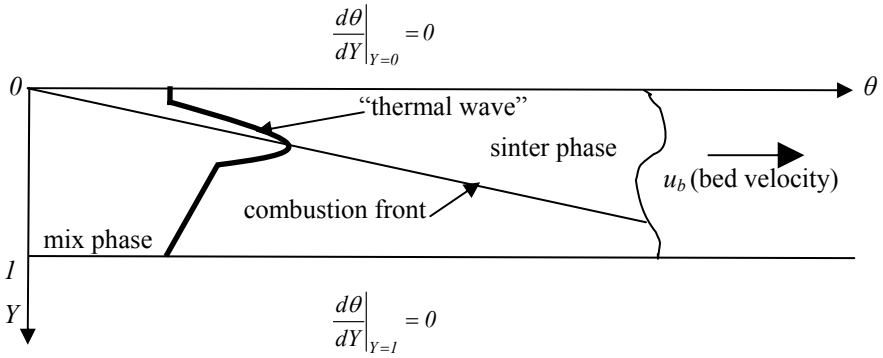

Figure 2 – Domain scheme and boundary conditions.

In order to obtain the thermal wave, it is used a one-dimensional transient model in porous medium and moving heat source, which main hypothesis is in accordance to Macedo (1998):

a) The humidity bed is considered constant and uniform;
b) The bed is considered an isotropic porous medium and its porosity (φ) is constant and uniform;
c) The porous matrix is constituted by two distinct phases: solid phase and fluid phase (gaseous);
d) The local average volume hypothesis is used to the developement of conservation equations;
e) The contact between solid phase and fluid phase is perfect, in such way that local thermal equilibrium is valid;
f) It is considered variations just on vertical bed direction and temporal (one-dimension transient problem);
g) Radiation heat transfer inside the porous matrix is neglected, as well as viscous dissipation effects and work realized by changes in the pressure field ;

h) Thermo-physical properties which varies with temperature are considered by its average values representative of sintering process;
i) Transport of humidity and vapor by diffusion are neglected;
j) It is not considered a pre-heating phase as well as the drying phase before combustion.
k) The simulated thermal profile consider a punctual, continuous and moving heat source, in such way to reproduce a decoupled temperature field, in relation to the gaseous emissions model, but compatible with typical sintering process.

4.1. Mathematical model for the thermal profile

The mathematical model for thermal wave considering the premises described above is composed by the following dimensionless governing Eq. (6).

$$\frac{\partial \theta_k(Y,\tau)}{\partial \tau} = \frac{\partial^2 \theta_k(Y,\tau)}{\partial Y^2} - V_{gk}\frac{\partial \theta_k(Y,\tau)}{\partial Y} + C_{mk}\, q'''_{móvel} \tag{6}$$

where *m* indicates mix phase, *g*, gaseous phase, *k=1* consider properties before combustion and *k=2*, properties after combustion. The dimensionless groups are defined in Eqs. (7a-c).

$$\tau = \frac{\alpha_s t}{L^2}\left(Fourier\ number\right) \qquad Y = \frac{y}{L} \qquad q'''_{movel} = q'''_m \delta(y - u_b.t)\text{, where } \delta \text{ is the Dirac delta} \tag{7a,b,c}$$

The definition of variables depends on the temporal position analyzed: before or after combustion front, as defined by Eqs. (8-11).

BEFORE COMBUSTION (*k=1*) AFTER COMBUSTION (*k=2*)

$$\theta_1(Y,\tau) = \frac{T_1(y,t) - T_\infty}{T_\infty} \qquad \theta_2(Y,\tau) = \frac{T_2(y,t) - T_\infty}{T_\infty} \tag{8a,b}$$

$$V_{g1}(Y) = \frac{\varphi_{mix} L(\rho c_p)_g}{k_{mix}}\vec{V}_1 \qquad V_{g2}(Y) = \frac{\varphi_{sinter} L(\rho c_p)_g}{k_{sinter}}\vec{V}_2 \tag{9a,b}$$

$$C_{m1} = \frac{L^2}{(\rho c_p)_{m1} T_\infty \alpha_{m1}} \qquad C_{m2} = \frac{L^2}{(\rho c_p)_{m2} T_\infty \alpha_{m2}} \tag{10a,b}$$

$$\alpha_{m1} = \frac{k_{m1}}{(\rho c_p)_{m1}}\left(Thermal\ difusivity\ of\ \ phase\ 1\right) \qquad \alpha_{m2} = \frac{k_{m2}}{(\rho c_p)_{m2}}\left(Thermal\ difusivity\ of\ \ phase\ 2\right) \tag{11a,b}$$

The model described by Eqs. (6-11) was solved via General Integral Transform Technique (*GITT*), considering the methodology established in Cotta (1993), Cotta and Mikhailov (1997) and a long list of thermal physical properties related by Young (1977) and Nath *et al.* (1997), Tab. (3), which fed a FORTRAN code written for this case. Altought it is not a more realistic representation of the thermal profile, the simulated curves in Fig. (3) were obtained for this case.

Table 3 - Main properties and parameters adopted for Eqs. (4-9), averaged from Young (1977), Nath *et al.* (1997) and CST data

Bed porosity		$\varphi = 0,4$	Aparent density of solids	$\rho_s = 4.572\ kg/m^3$
Average temperature of solids		$T_s = 1.523,15\ K$	Aparent density of bed	$\rho_l = 2.743,2\ kg/m^3$
Average temperature of gas		$T_g = 800\ K$	Specific flux mass	$\dot{m} = 0,2166\ [kg/m2/s]$
Bed dimensions	Height	$L = 0,4\ m$		
	Width	6,00m	Average pellet diameter	$dp = 3mm$
	Lenght	80,00m	Specific heat of solids	$c_s = 1,28\ kJ/kg.K$
Specific mass of coke		$\rho_c = 1.200\ kg/m^3$	Specific heat of gas	$c_g = 1,10\ kJ/kg.K$
Specific mass of limestone		$\rho_{cal} = 1.600\ kg/m^3$	Thermal conductivity of solids	$k_s = 6,50\ W/m.K$
Specific mass of iron ore		$\rho_{min} = 5.200\ kg/m^3$	Thermal conductivity of gas	$k_g = 0,073\ W/m.K$
Specific velocity of gas		$V = 1,10\ m^3/s/m^2$	Thermal conductivity of bed	$k_l = 3,93\ W/m.K$
Specific area of pellets		$a = 1.200$	Gas density	$\rho_g = 0,43\ kg/m^3$
Pressure drop in bed		$\Delta P = 12\ kPa$	Gas viscosity	$\mu = 1,72\ x10^{-6}\ kg/m.s$
Processing time		t =34,81min	Coke mass fraction	$M_c = 0,04$
Bed velocity		u_b= 0,04 m/s	Limestone mass fraction	$M_{cal} = 0,13$

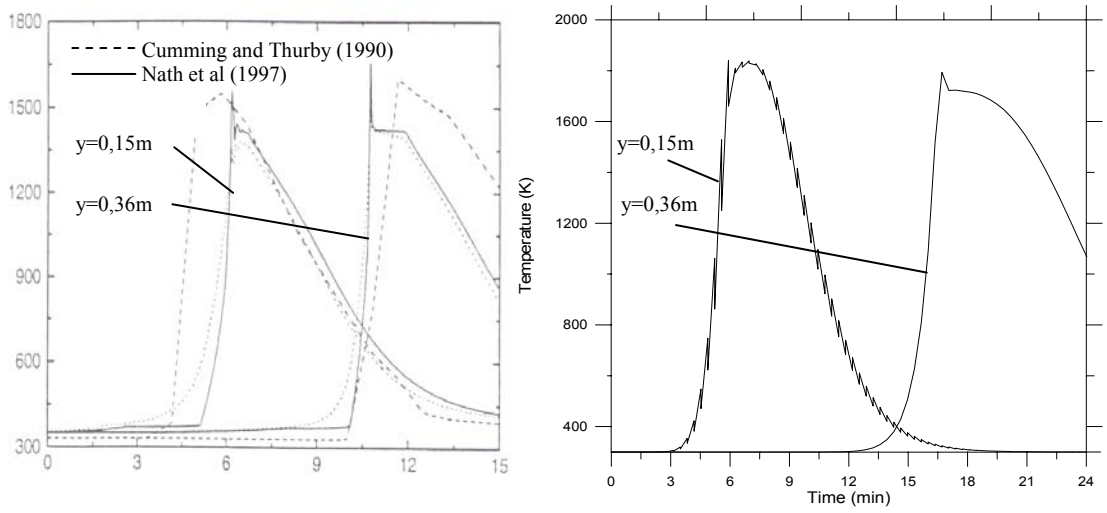

(a) (b)

Figure 3 - (a) "Thermal wave" obtained by Nath *et al.* (1997); (b) Thermal wave simulated by present model (AC/AH/AO/AN = 2/2/23/74)

An analysis of Fig. (3) indicates that, although they are very approximated when compared one to each other, there are quantitative differences between the thermal profile from the reference (Fig. 3a) and that obtained by the present model (Fig. 3b). On the other hand, it is evident the qualitative similarity between those curves, including the temperature peak, typical of combustion process. Such behavior is analog for two bed depth analyzed: *y=0.15* and *y=0.36m.* Although it is not represent the more realistic behavior of the phenomenon, such results were considered as appropriated for the purposes of the present study.

5. Applying the thermal wave to the emissions model

In order to check the proceeding, which consists to apply the thermal wave model to the emissions model, it was simulated the problem presented in Nath *et al.* (1997) and Cumming e Thurlby (1990) for the prediction of sintering bed emissions. The comparison for CO_2, H_2O, O_2 and CO emissions are demonstrated in Figs. (4).

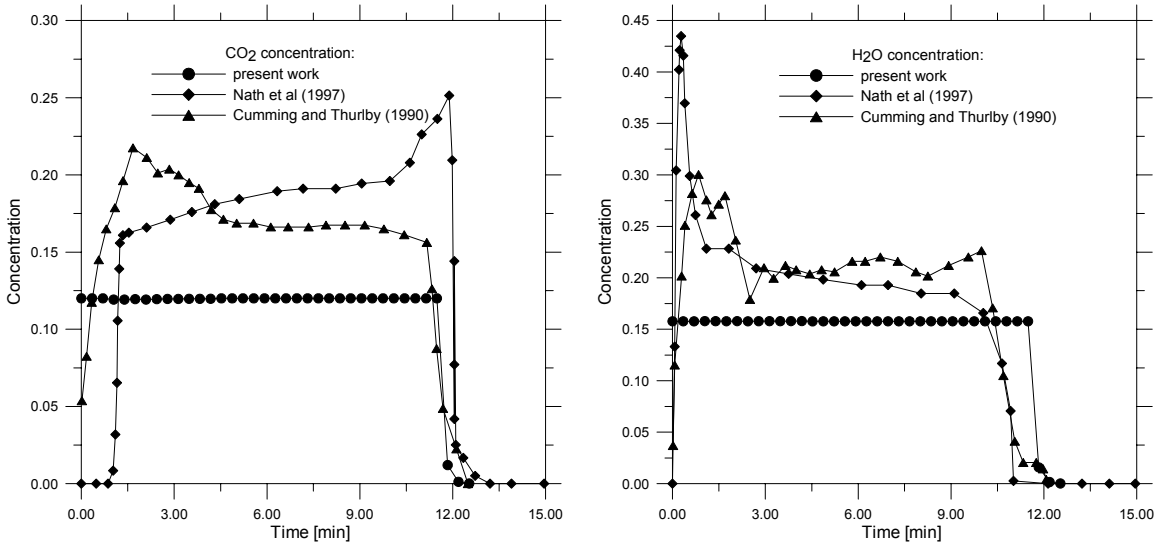

(a) (b)

Figure 4 - (a) CO_2 concentration comparison: Nath et al. (1997), Cumming and Thurlby (1990) and present work ; (b) H_2O concentration comparison: Nath et al. (1997), Cumming and Thurlby (1990) and present work

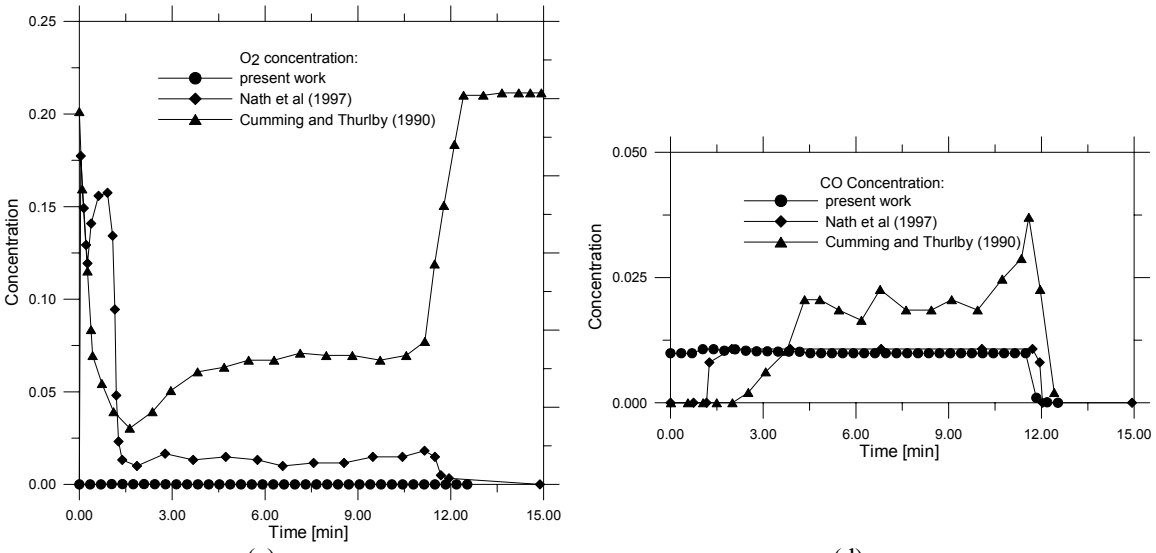

(c) (d)

Figure 4 - (c) O_2 concentration comparison: Nath et al. (1997), Cumming and Thurlby (1990) and present work ; (d) *CO* concentration comparison: Nath et al. (1997), Cumming and Thurlby (1990) and present work

An analysis of Fig. (4) indicate that, from a qualitative point of view, there are good agreement between the results of references and the results from the present work. Discrepancies in quantities are observed, although the order of magnitude is preserved. Such discrepancies are observed between the own authors as well and it can be explained when is considered that the references were produced using kinetic reactions approach, instead of chemical equilibrium model. Moreover, the problem solved by references predicts the emission of 5 species (CO_2, CO, O_2, H_2, H_2O) against 10 species predictable by the present model (CO_2,, CO, O_2, O, NO, N_2, H, H_2, OH, H_2O) so, consuming much more O_2 which may explain the absence of oxygen in Fig. (4c) in present simulation.

From previous observations, it was considered that the model composed by the thermal wave coupled to the chemical equilibrium approach, proposed here reaches reasonable results, appropriated to the purposes of the present work.

6. The methodology for gaseous emissions prediction in sintering bed

CST company use to measure two gas species for its sintering machine chimney: *CO* and *NO*. The methodology to predict emissions produced by sintering process, proposed in this work, is based on the adjustment of air quantity (air excess - Δair) used in the combustion process. This adjustment is obtained from the comparison between the concentrations of *NO* and *CO* simulated by the model and the actual emissions measured in CST. So, a given value of air excess that leads to an acceptable concordance between the simulated and actual emissions in a given period of time, is used for simulate the prediction emissions in the future. This procedure is the essence of the present methodology.

In order to proceed with such methodology, it is defined the concentrations of C/H/O/N in fuel composition considering that all oxygen necessary for the combustion process come from atmosphere, originating the relations of Eq. (12a-d), proportional to the concentrations of atmospheric air.

$$AC = AC + (\Delta_{air} * 0{,}00734) \tag{12a}$$

$$AH = AH + (\Delta_{air} * 0{,}13946) \tag{12b}$$

$$AO = AO + (\Delta_{air} * 0{,}1897485) \tag{12b}$$

$$AN = AN + (\Delta_{air} * 0{,}6634517) \tag{12b}$$

Now, the code must be fed with process parameters from company machine and all of such parameters have to be translated to a molar basis system, as well as all input parameters (fuel consumption, fuel composition, mix composition, gas exhaustion flux, etc). The mix piles and the fuel composition are programmed for some weeks in advance by sintering operation staff. These parameters as well as all others related to the sintering machine was provided by CST and are not be listed here for a matter of synthesis, but it can be found in Silva, R.H.B. (2005).

All quantities were converted to daily averaged values and weighted-up to the quantity equivalent to burn one bed volume of mixture, following the steps described by Silva, R.H.B. (2005).

The sintering bed characteristics, as defined in Tab. (3) and the production weeks of *CST*, selected to be analyzed are listed in Tab. (4), were used for all simulations reported.

Table 4 – Selected production weeks (year: 1999)

Week n.	Period of time
1	18 to 24 / June
2	23 to 29 / September
3	01 to 08 / November
4	09 to 15 / November
5	02 to 08 / October
6	09 to 15 / October

Among some others tentative to adjust the value of Δ_{air} in order to simulate the emissions of *CO* and *NO*, it will be described only the successfully one that consists to find the value of Δ_{air} which best fit the simulated to the actual *CO* emissions, as well as another value of Δ_{air} which best fit the simulated to the actual *NO* emissions for a given date. The two values were averaged to get a Δ_{air} medium value. The result of such adjustment is showed in Figs. (5) to four weeks as an exemplification.

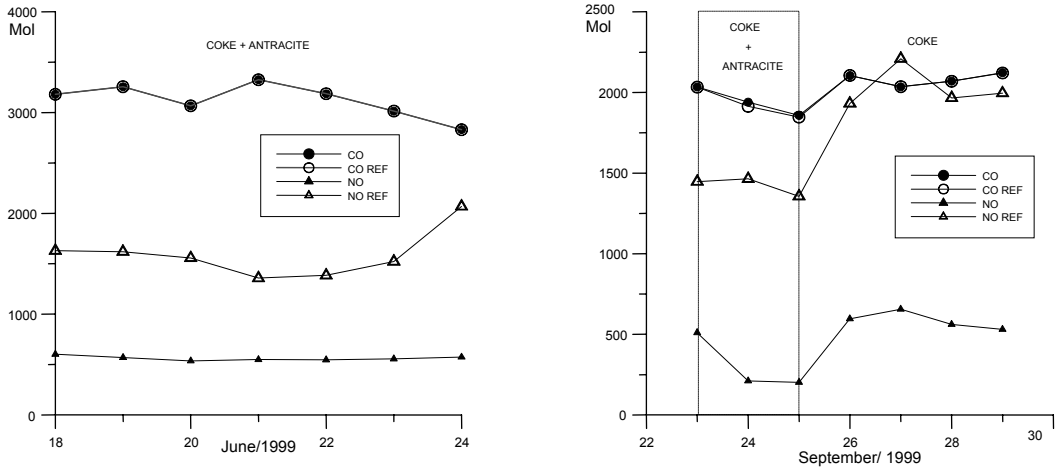

(a) (b)

Figure 5 – a) Simulated and measured (ref.) curves of *CO* and *NO* emissions for week 1;
b) Simulated and measured (ref.) curves of *CO* and *NO* emissions for week 2.

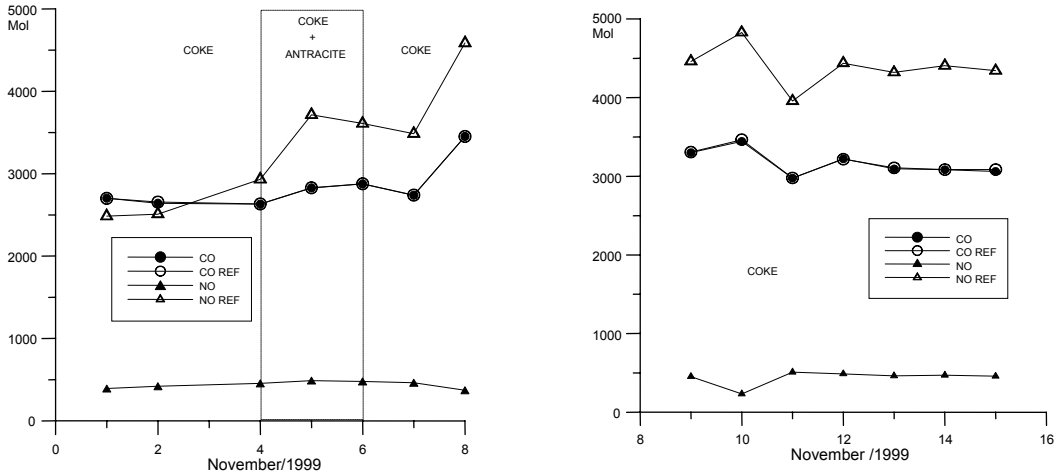

(c) (d)

Figure 5 – c) Simulated and measured (ref.) curves of *CO* and *NO* emissions for week 3;
d) Simulated and measured (ref.) curves of *CO* and *NO* emissions for week 4.

7. Results and discussions

The averaged value of Δ_{air} is now used to run the code but now, it is fed with fuel composition programmed in future and, so, predicting the emissions there. In Figs. (6) this procedure was made to check the prediction emission quality in time.

Figure (6a) shows the predictions with one week in advance. As evidenced, the *NO* approximation is better than *CO*, although it has some days when the predictions almost coincide with the measured concentrations, as show the simulations for 11-15 days. Figure (6b) show the average difference between simulated and measured emissions of *CO* is 3,35% and 0,48% for *NO*.

Such behavior is observed in Fig. (6c,d) as well, but in this case for a prediction of two weeks in advance. In Fig. (6c) the concordance of *NO* is better than *CO* prediction again and the difference between them (Fig. (6c)) tends to increase for *CO* prediction but show an unexpected decreasing for *NO* prediction.

The deterioration of the results becomes more evident for a prediction with four weeks in advance, as show in Fig. (6e,f) where the difference between simulated and actual emissions reach more than 10% for *CO* prediction, although the *NO* prediction still retain good agreement (difference about less than 0,5%).

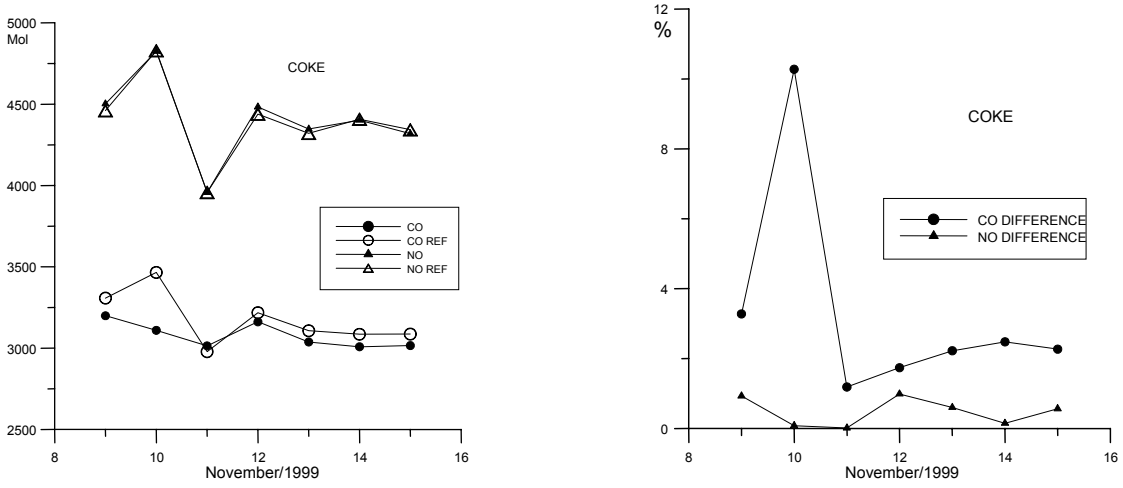

(a) (b)

Figure 6 - Predictions of *CO* and *NO* emissions for one week in advance (week 4 adjusted with Δair from week 3): a) Comparison between predictions and actual emissions (ref.); b) Differences between prediction and actual emissions (average difference of 3,35% for *CO* and 0,48% for *NO*)

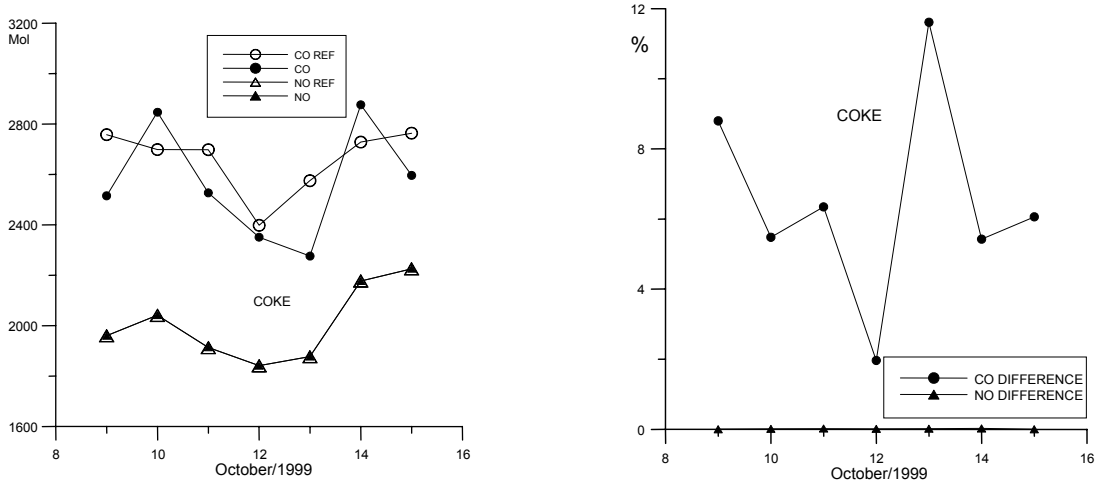

(c) (d)

Figure 6 - Predictions of *CO* and *NO* emissions for two weeks in advance (week 6 adjusted with Δair from week 2): c) Comparison between predictions and actual emissions (ref.); d) Differences between prediction and actual emissions (average difference of 6,52% for *CO* and 0,014% for *NO*)

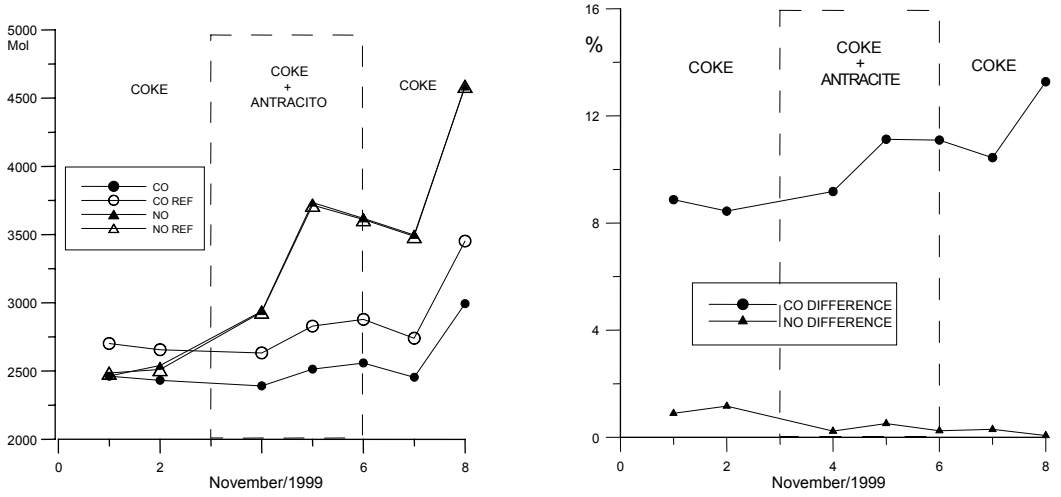

(e) (f)

Figure 6 - Predictions of *CO* and *NO* emissions for four weeks in advance (week 3 adjusted with Δair from week 2): e) Comparison between predictions and actual emissions (ref.); f) Differences between prediction and actual emissions (average difference of 10,35% for *CO* and 0,49% for *NO*)

Now, it is convenient to show the emissions of other gas species predictable by the chemical equilibrium computational code as CO_2, O_2, N_2 , H_2O, CO, NO_2,, H_2 , OH, O and H as shown in Fig. (7a-c), which are presented in distinct plots due to scale matter. In this case, there is no comparison with actual data, since the company does not monitor such gases, but the validation of such emissions was justified in section (5).

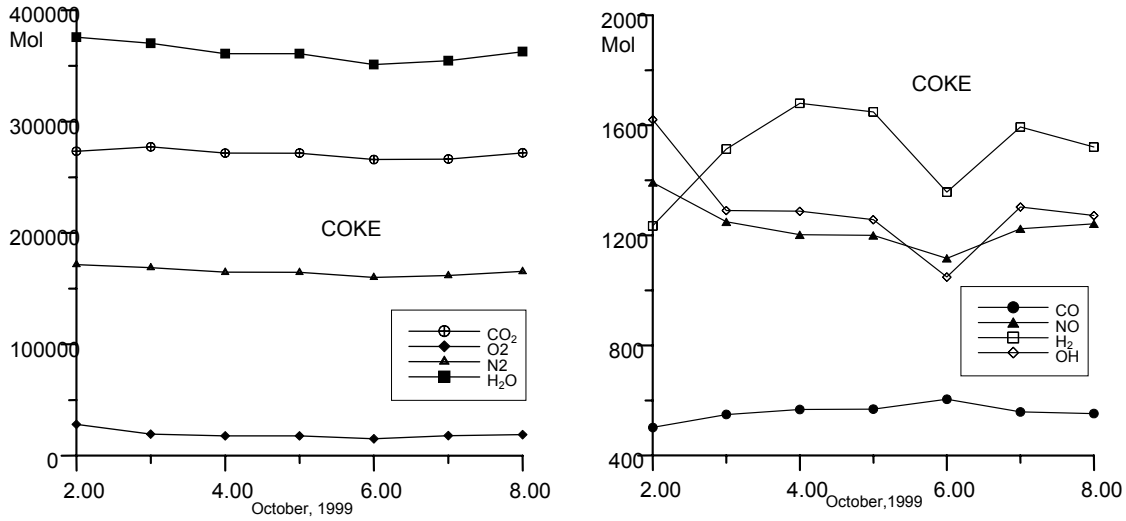

(a) (b)

Figure 7 - Predictions for week 5: a) Predictions of CO_2, O_2, N_2 and H_2O; *b)* Predictions of CO, NO_2,, H_2 and OH

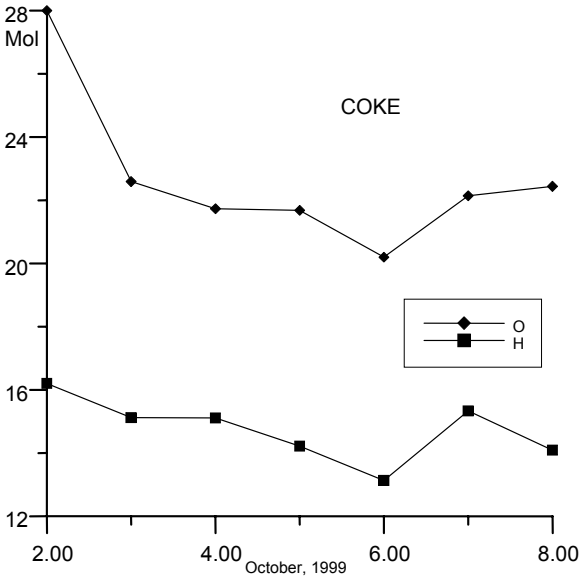

(c)

Figure 7 - Predictions for week 5: c) Predictions of *O* and *H*

As can be inferred from the results, the present proposition seems to predict satisfactorily the emissions of the model, since the prediction do not exceed two or four weeks in advance.

In reality, the parameter that corresponds to the air excess (Δ_{air}) loses its strict sense and includes all errors of the model due to the adopted approximations for the gaseous formation and thermal wave. So, this parameter include operational variations not predictable by modeling, like: a) uniformity lack in mix and fuel composition; b) humidity variation of mix piles, due to seasonality of rain and dry seasons; c) differences between estimated and actual thermo-physical properties and the air excess properly said.

Once properties estimative and other approximations becomes more realistic and fed the computational code, this parameter tends to fit to the actual air excess used in the combustion process.

It is possible, in the future, to include the influence of new gas monitoring emissions since the appropriated sensors are installed in the chimney. To proceed this, the methodology has to consider this new measurements in the procedure to averaging Δ_{air} value, as described in section (6).

8. Acknowledgements

The authors would like to express their acknowledgements to the Mechanical Engineering Post-Graduation Program - PPGEM/UFES, for the use of its facilities and *Companhia Siderúrgica de Tubarão - CST*, for partial financing this work as well as the cession of its sintering process data.

9. References

Campbell, A. S., 1979. "Thermodynamic Analysis Of Combustion Engines". John Wiley & Sons, New York.

Cotta, R.M., 1993. "Integral Transforms in Computational Heat and Fluid Flow", CRC Press, Boca Raton, Fl.

Cotta, R.M. and Mikhailov, M.D., 1997.,"Heat Conduction – Lumped Analysis, Integral Transforms, Symbolic Computation", Wiley Interscience, New York.

Cumming, M. J.; Thurlby, J. A., 1978, "Developments in modeling and simulation of iron ore sintering". Ironmaking and Steelmaking 1, pp. 25-31.

Dash, I. R.; Rose, E., 1978. "Simulation of a sinter strand process". Ironmaking and Steelmaking 5, pp. 25-31.

Dias, L.A.M., 1998. Estruturas de aço: conceitos, técnicas e linguagem", 2. ed. São Paulo, Zigurate Editora, 159p, São Paulo.

Macêdo, E. N.,1998, "Simulação computacional e estimativa de propriedades termo-físicas na combustão de troncos cilíndricos de madeira". Rio de Janeiro, 226 p. Tese de Doutorado – Faculdade de Engenharia Mecânica, Universidade Federal do Rio de Janeiro.

Muchi, I.; Higuchi, 1972, "Theoretical analysis of sintering operation", Journal of Transactions Iron Steel Institute Japan 12, pp. 54-63.

Nath, N. K.; Da Silva, A. J.; Chakraborti, N., 1997, "Dynamic process modeling of Iron ore sintering". Steel Research 68 (7), pp. 285-292.

Silva, R.H.B., 2005, "Uma metodologia para previsão de emissões em leito de sinterização utilizando dados de processo", Vitória, 122p. Tese de Mestrado - Programa de Pós Graduação em Engenharia Mecânica, Universidade Federal do Espírito Santo.

Yoshinaga, M. and Kubo, T., 1978, "Approximate simulation model for sintering process", Sumitomo Search 20, pp.1-14.

Young, R. W., 1977, "Dynamic mathematical model of sintering process". Ironmaking and Steelmaking 6, pp. 321-328.